Implementation of blob basis functions in proton CT reconstruction

H. Heaton[†], C. Ordonez[§], Y. Censor[ℒ], R. Schulte[‡]

[†]Walla Walla University, [§]Northern Illinois University, [ℒ]University of Haifa, [‡]Loma Linda University

The Key Question

In proton computed tomography (pCT), will use of Kaiser-Bessel window functions (often called 'blobs') improve image reconstruction quality over that of a corresponding voxel basis?

Introduction

Blob basis functions yield promising results in multiple imaging modalities and we seek to test their use in proton CT (pCT). Unlike the straight-line approximations in x-ray CT, in pCT discrete steps along a most likely path formalism of the nonlinear paths of Coulomb-scattered protons is used. Below is an illustration of the basis functions of interest. Voxels have a uniform value inside a set domain while blobs are spherically symmetric and taper smoothly to zero at their border.

Figure 1: Profile of a voxel (a) and a blob (b)

Series Expansion Representation

Series expansion methods assume that a 3D image can be represented using a linear combination of a set $\{b_j\}$ of fixed basis functions. An approximation f^* of an image f is defined at a position $\vec{r} \in \mathbb{R}^3$ by

$$f(\vec{r}) \approx f^*(\vec{r}) = \sum_j \vec{x}_j \cdot b_j(\vec{r}) \qquad (1)$$

where b_j denotes the jth basis function and each entry x_j of the vector $\vec{x}$ gives a weighting factor for the contribution of b_j. For a set of basis functions, the estimate f^* is uniquely determined by the entries of $\vec{x}$, which is called the image vector.

pCT Image Reconstruction Problem

The water equivalent path length (WEPL) traveled by each proton through an object can be expressed as a line integral of relative (to water) stopping powers (RSP) along the path. In practice, these integrals are expressed as discrete sums, which leads to the linear system

$$A\vec{x} = \vec{y}. \qquad (2)$$

The ij-th entry of A gives the intersection length of the i-th proton through the j-th basis function and the i-th entry of the measurement vector $\vec{y}$ gives the i-th proton's measured WEPL. The CT reconstruction problem is:

$$\textbf{Given } A \textbf{ and } y\textbf{, estimate } x. \qquad (3)$$

Assigning Intersection Lengths

To generate A, which is called the system matrix, the path length through each basis function must be computed. Employing a linear path approximation through individual basis functions allows the Radon transform to approximate each entry A_{ij}, i.e.,

$$A_{ij} = \int_{path} b_j(\vec{s})\, d\vec{s} \approx [\mathcal{R}b_j](\ell_i, \theta_i) \qquad (4)$$

where

$$[\mathcal{R}b_j](\ell_i,\theta_i) = \int_{line} b_j\left(\sqrt{\ell_i^2 + z^2},\ \theta_i + \tan^{-1}(z/\ell_i)\right)\, dz.$$

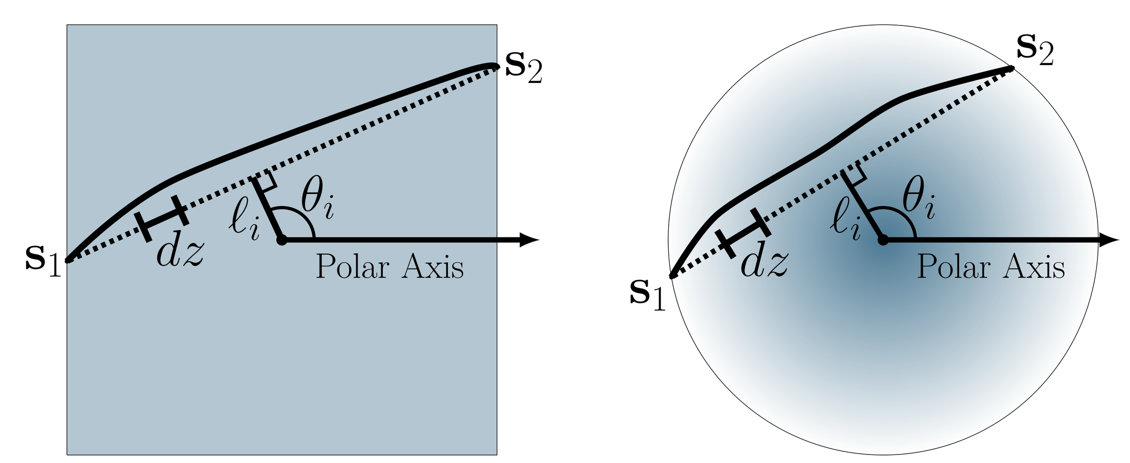

Figure 2: Illustration of Radon transform for voxels (left) and blobs (right)

Note the Radon transform is simply the geometric path length with voxels. Due to symmetry, with blobs this transform is dependent solely on the perpendicular distance ℓ_i of the linear approximation from the blob center.

Generating the System Matrix

Below we outline an algorithm to identify each nonzero blob intersection length. This is illustrated in Figure 4. Step 1 identifies a blob in proximity to $\vec{\varphi}^\ell$. Step 3 begins a loop to cycle through additional nearby blobs within a chosen range κ. Step 6 restricts intersection lengths to being assigned during the last step the proton takes before passing the blob center in depth.

1: $\vec{\Phi}^\ell \leftarrow \left(\lfloor(\vec{\varphi}^\ell)_x/\beta\rfloor,\ \lfloor(\vec{\varphi}^\ell)_y/\beta\rfloor,\ \lfloor(\vec{\varphi}^\ell)_z/\beta\rfloor\right)$
2: $\vec{\mu}^\ell \leftarrow \vec{\varphi}^{\ell+1} - \vec{\varphi}^\ell$
3: **for** $(m,n,p) \in \mathbb{Z}^3$ with $0 \le |m|, |n|, |p| \le \kappa$ **do**
4: **if** $m + (\vec{\Phi}^\ell)_x \equiv n + (\vec{\Phi}^\ell)_y \equiv p + (\vec{\Phi}^\ell)_z \pmod 2$
5: $\vec{\nu}^{j\ell} \leftarrow \beta \cdot (\vec{\Phi}^\ell + (m,n,p)) - \vec{\varphi}^\ell$
6: **if** $|\vec{\nu}^{j\ell}| \le a$ **and** $\vec{\nu}_u^{j\ell} \in [0, s)$
7: $\vec{\tau}^{j\ell} \leftarrow \vec{\nu}^{j\ell} - \dfrac{\langle \vec{\nu}^{j\ell}, \vec{\mu}^\ell\rangle}{\langle \vec{\mu}^\ell, \vec{\mu}^\ell\rangle} \cdot \vec{\mu}^\ell$
8: Use (m,n,p) and $\vec{\Phi}^\ell$ to identify index j
9: $A_{ij} \leftarrow [\mathcal{R}b_j]\left(|\vec{\tau}^{j\ell}|\right)$
10: **end if**
11: **end if**
12: **end for**

Algorithm 1: Steps computed for each point $\vec{\varphi}^\ell$.

Our Algorithmic Task

To compare voxel and blob-based proton CT image reconstructions, we first must solve the following problem:

Let $\{\vec{\varphi}^\ell\}_{\ell=1}^L$ denote an ordered set of points along a path in $\mathbb{R}^3$. Suppose this path passes through an object, which is to be represented with a set $\{b_j\}$ of blob basis functions. Using successive points $\vec{\varphi}^\ell$ along the path, uniquely estimate each nonzero blob intersection length of the path to generate the corresponding system matrix.

Identification of Blobs in a Proximity

A key step in our algorithm is to identify blobs within a given proximity of a point $\vec{\varphi}^\ell$. We do this by identifying a corresponding point $\vec{\Phi}^\ell$ located nearby on the grid on which the blobs are centered.

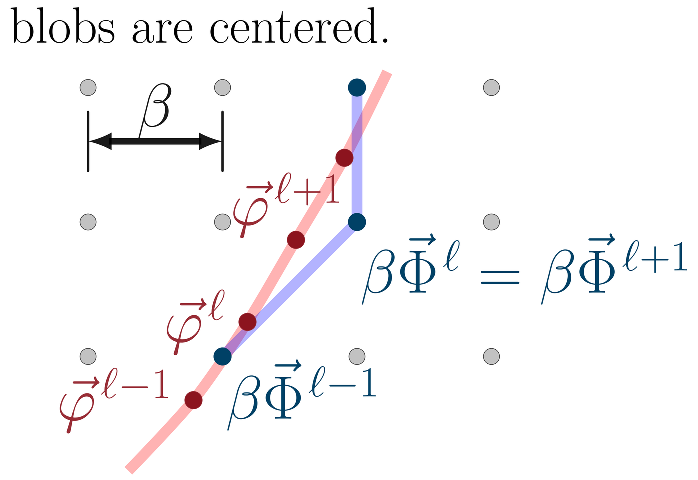

Figure 3: Schematic 2D illustration of the relation between $\vec{\varphi}^\ell$ (red) and $\vec{\Phi}^\ell$ (blue). Each $\vec{\varphi}^\ell$ is mapped rightward and upward to get the corresponding $\beta\vec{\Phi}^\ell$.

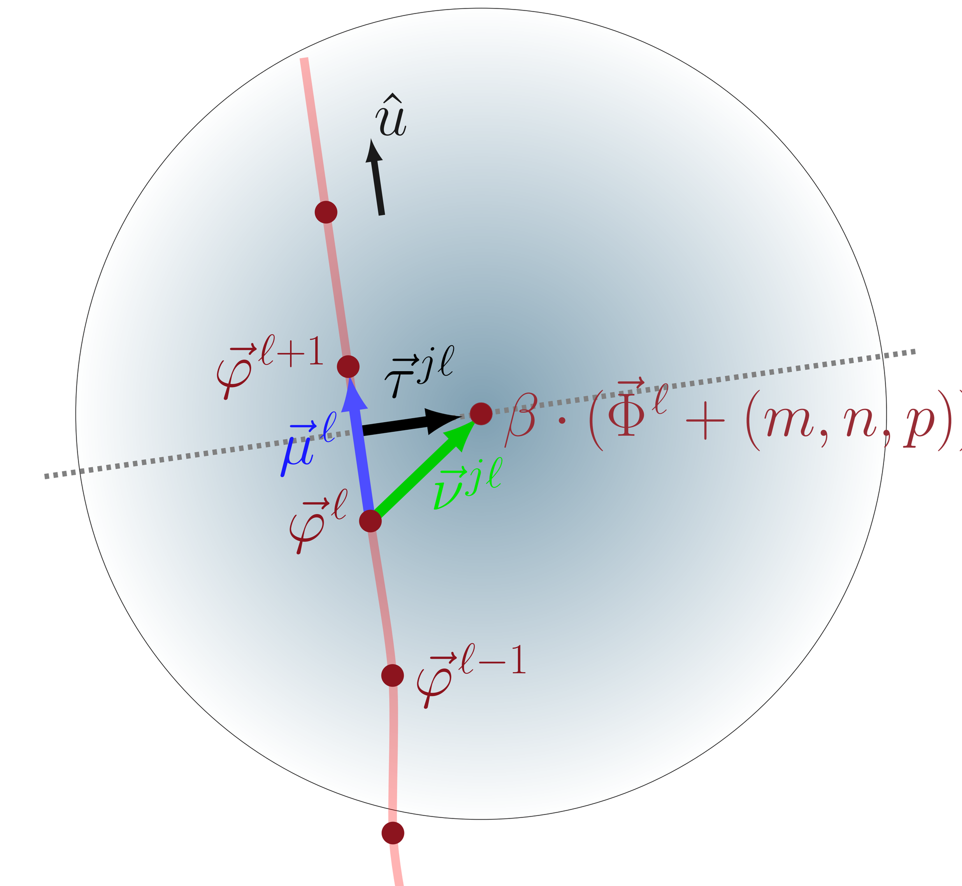

Figure 4: Illustration of Algorithm 1

Preliminary Results

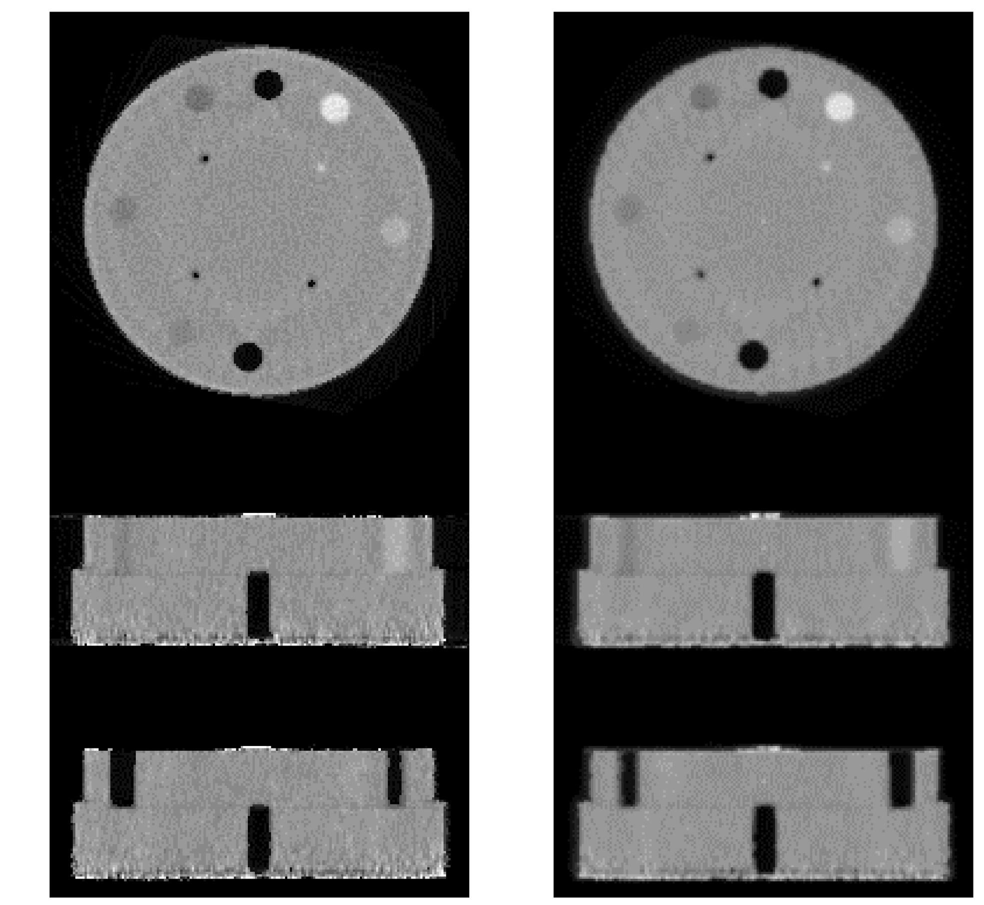

(a) Voxel-Based (b) Blob-Based

Figure 5: Proton CT reconstructions of a cyldindrical phantom with experimental data. Reconstruction with voxels (a) used a constant chord length and that with blobs (b) used Algorithm 1 with exact chords.

Planned Experiment

Simulating pCT data with GEANT4, we will quantitatively compare voxel and blob-based reconstructions using a modified form of the γ index function used in radiology. We hypothesize blobs will yield results with image reconstruction quality superior to those with voxels.

References

[1] S. Agostinelli et al. Geant4 – a simulation toolkit. *Nuclear Instruments and Methods in Physics Research A.* 506 (2003), 250-303.

[2] G.T. Herman. *Fundamentals of Computerized Tomography: Image Reconstruction from Projections,* Springer-Verlag, London, UK, 2nd Edition, 2009.

[3] S. Matej and R.M. Lewitt. *Practical considerations for 3-D image reconstruction using spherically symmetric volume elements,* IEEE Transactions on Medical Imaging, 15 (1996), 68-78.

Acknowledgements

We wish to thank Dr. Gabor Herman at City University of New York and Dr. Keith Schubert and Blake Schultze M.S. from Baylor University for useful discussions. This work was supported by Research Grant No. 2013003 of the United States-Israel Binational Science Foundation (BSF). Howard Heaton's work on this project was supported by Loma Linda University School of Medicine's Biomedical Undergraduate Research Program and the American Association of Physicists in Medicine's DREAM Fellowship.